This article was downloaded by: [Tomsk State University of Control Systems and Radio]
On: 18 February 2013, At: 10:39
Publisher: Taylor & Francis
Informa Ltd Registered in England and Wales Registered Number: 1072954 Registered office: Mortimer House, 37-41 Mortimer Street, London W1T 3JH, UK

Molecular Crystals and Liquid Crystals Science and Technology. Section A. Molecular Crystals and Liquid Crystals

Publication details, including instructions for authors and subscription information:
http://www.tandfonline.com/loi/gmcl19

Growth Defect Studies in SiC Single Crystals

Michael Dudley [a] & William M. Vetter [a]

[a] Dept. of Materials Science & Engineering, SUNY at Stony Brook, Stony Brook, NY, 11794-2275, USA

Version of record first published: 24 Sep 2006.

To cite this article: Michael Dudley & William M. Vetter (1996): Growth Defect Studies in SiC Single Crystals, Molecular Crystals and Liquid Crystals Science and Technology. Section A. Molecular Crystals and Liquid Crystals, 278:1, 37-46

To link to this article: http://dx.doi.org/10.1080/10587259608033655

PLEASE SCROLL DOWN FOR ARTICLE

Full terms and conditions of use: http://www.tandfonline.com/page/terms-and-conditions

This article may be used for research, teaching, and private study purposes. Any substantial or systematic reproduction, redistribution, reselling, loan, sub-licensing, systematic supply, or distribution in any form to anyone is expressly forbidden.

The publisher does not give any warranty express or implied or make any representation that the contents will be complete or accurate or up to date. The accuracy of any instructions, formulae, and drug doses should be independently verified with primary sources. The publisher shall not be liable for any loss, actions, claims, proceedings, demand, or costs or damages whatsoever or howsoever caused arising directly or indirectly in connection with or arising out of the use of this material.

Mol. Cryst. Liq. Cryst., 1996, Vol. 278, pp. 37–46
Reprints available directly from the publisher
Photocopying permitted by license only

© 1996 OPA (Overseas Publishers Association)
Amsterdam B.V. Published in The Netherlands
under license by Gordon and Breach Science
Publishers SA
Printed in Malaysia

GROWTH DEFECT STUDIES IN SiC SINGLE CRYSTALS

MICHAEL DUDLEY AND WILLIAM M. VETTER
Dept. of Materials Science & Engineering, SUNY at Stony Brook, Stony Brook, NY 11794-2275, USA

Abstract Growth defects in vapor grown 6H-SiC single crystals have been studied using a combination of techniques, including: synchrotron white beam x-ray topography (SWBXT), conventional optical microscopy, fluorescence microscopy, and epi-fluorescence laser scanning confocal microscopy (LSCM). These studies of crystal sections cut both parallel and perpendicular to the [0001] growth axis focused on growth dislocations of screw character running approximately parallel to the growth axis. SWBXT back-reflection and transmission images are presented of these dislocations, which are known to possess a range of Burgers vector magnitudes, and in the case of large Burgers vector magnitude, hollow cores, known as micropipes. Results of detailed LSCM and fluorescence microscopy imaging of these micropipes are presented and discussed in the light of the SWBXT images.

Detailed SWBXT studies further reveal that slip dislocations lying in the (0001) plane are connected to the growth dislocations, and appear to emanate from them, periodically along their lengths, in the form of loops. The periodicity, along the superscrew dislocations, of these dislocation generation phenomena, is found to be very similar to the periodicity of dilation and constriction phenomena in the associated micropipes, as measured by LSCM and fluorescence microscopy. This suggests that the two phenomena may be related.

INTRODUCTION

It is widely recognized that many crystals grown from the vapor or solution phase can grow by a screw dislocation mechanism and may exhibit growth spirals on their surfaces[1]. In the cases of polytypic substances, such as SiC or CdI_2, these spirals are often of quite large step heights, implying dislocations of giant Burgers vectors, multiples of the *c* lattice parameter. Indeed, x-ray topographic images reveal the existence of dislocations of such character,[2–7] which, due to their large Burgers vectors, have been termed superscrew dislocations. Typically, at the centers of such spirals and extending downward through the length of the crystal in its *c*-direction, a hollow tube, or micropipe, is observed, considered to coincide with the core of the superscrew dislocation.

Downloaded by [Tomsk State University of Control Systems and Radio] at 10:39 18 February 2013

Downloaded by [Tomsk State University of Control Systems and Radio] at 10:39 18 February 2013

Considerable progress in the understanding of the nature and implications of these superscrew dislocations was achieved through the work of Frank. After his proposal of the screw dislocation theory of crystal growth,[8] Frank extended the idea to the formation of polytypes.[9] In his thinking, a screw dislocation created in an initial platelet of a thermodynamically stable phase of SiC such as 6H, 15R or 4H gives rise to a perpetual step which winds up through the length of the crystal during further growth to form the polytypic phase with an axial repeat distance equal to the dislocation Burgers vector. Frank also proposed a theory predicting the formation of the hollow cores, where the surface energy of the micropipe forms an equilibrium with the dislocation's strain energy at a certain diameter in relation to its Burgers vector.[10] Frank's theory of polytype formation was subsequently modified to include the expansion of basal plane stacking faults which, when aided by the presence of the original screw dislocation, can lead to the formation of related polytypes via what is referred to as a periodic slip process.[11] Frank's mechanism of spiral growth around a screw dislocation remains central to this modified theory.

Over a period spanning almost five decades, various attempts at detailed characterization of superscrew dislocations in SiC have been reported. For example, superscrew dislocation Burgers vectors have been obtained via measurement of step heights in growth spirals associated with individual dislocations using optical interferometry[1,12–14] and atomic force microscopy.[14] Of these, the optical technique appeared to give the most reliable results.[14] Burgers vectors have also been measured using x-ray topography.[3] Micropipe diameters have been measured using transmission optical microscopy of thin sections,[12] phase contrast microscopy,[15] x-ray topography,[3] and scanning electron microscopy (SEM).[6,13] In the case of the x-ray topographic diameter measurements, values obtained from the bulk of the crystal were a factor of ten times larger than those measured optically on the growth surface. This was interpreted as being due to a real difference between internal and as-grown surface diameters. However, detailed topographic analysis carried out in this laboratory indicates that the topographic measurement of micropipe diameter can significantly overestimate the value.[16]

On transmission optical micrographs of micropipes recorded from thick (a few hundred μm) SiC sections, the contrast of these cylindrical voids has always been faint.[6,7,17] Indeed, in our laboratory, we have often found that the easiest way to locate one of these micropipes is by the presence of its shadow falling across an unpolished face of a wafer, although diameter measurement is not feasible due to lack of definition in such images. To obtain micrographs showing higher contrast

Downloaded by [Tomsk State University of Control Systems and Radio] at 10:39 18 February 2013

and detail, we have borrowed a method used in the petrography of geomaterials such as sandstone.[18] The porous structures of such rocks have been studied by laser scanning confocal microscopy (LSCM) after infiltrating them with a low-viscosity epoxy containing a fluorescent dye. In this way it has been possible to "stain" the micropipes rendering them much more visible both in fluorescence and conventional optical microscopies. Details of their structures and shapes are revealed, and their dimensions can be measured accurately, using LSCM and other, less sophisticated, fluorescence microscopies. This will enable us to compare measurements of local micropipe diameter obtained using these optical techniques with observations of the detailed strain distribution and dislocation microstructure surrounding the micropipes obtained by synchrotron white beam x-ray topography (SWBXT). It also allows the validity of the Frank relationship between Burgers vector magnitude and micropipe diameter[10] to be tested, in principle enabling one to determine the minimum value of Burgers vector magnitude above which hollow cores are predicted to exist. This is crucial information for crystal growers since the number and size of micropipes can exert a strong influence over the yield of electronic devices fabricated from this material. The detailed analysis of the Frank relationship will be the subject of a separate paper.[19] In this paper we will present the methodology adopted for micropipe analysis. Examples of epi-fluorescence LSCM images and fluorescence microscopy images of micropipes in various geometries will be presented and compared with both conventional optical microscopy images and SWBXT images of the same micropipes. The morphology of the micropipes in relation to the local strain distribution and microstructure will be presented.

EXPERIMENTAL

Topographs were obtained by allowing the highly collimated, area-filling beam of synchrotron white x-rays obtained from beamline X19-C (the Stony Brook Synchrotron Topography Station) at the National Synchrotron Light Source, Brookhaven National Laboratory, to fall onto the silicon carbide wafers, while recording the area-filling diffracted beams on 8x10" sheets of Kodak Industrex SR-5 film placed normal to the incident beam direction at a distance of 10cm from the crystal.

LSCM samples were prepared by dissolving a red dye, rhodamine 6G in an epoxy with a viscosity of 60cP. The fluid was forced under 1atm. of pressure into the micropipes in a commercial basal-cut 6H-SiC wafer manufactured by Cree Research, Inc. The epoxy was then cured into a hard embedding material. Samples were cut free from the embedding block and the surfaces were prepared by mechanical

Downloaded by [Tomsk State University of Control Systems and Radio] at 10:39 18 February 2013

polishing down to a thickness of ca. 150μm. Longitudinal-cut samples were prepared by cementing a portion of this sample between two glass slides and sectioning it along the $(10\bar{1}0)$ plane with a low-speed diamond saw, followed by mechanical polishing down to a thickness of ca. 80μm. LSCM was performed with a Bio-Rad MRC-600 Confocal Imaging System attached to the side port of an inverted optical microscope (Nikon Diaphot). A krypton-argon laser(15mW) was used as a light source, with a 568nm excitor filter and YHS (rhodamine) filter block. The computations and images were made with the use of VoxelView/Ultra2.1 (Vital Images, Fairfield, IA) on a Silicon Graphics XS24 workstation.

RESULTS AND DISCUSSION

LSCM has been used extensively in the biological sciences but has only seen limited application in the materials sciences. The current state of the technology of this method allows precise control of the lateral (x-y) coordinates of the laser and axial (z) position of the stage, and also enables automatic rapid processing as the laser is scanned across the field of view, through interfacing the microscope with a computer. Since each point on a specimen may be illuminated and detected individually, without light scattered from neighboring points, x-y resolution to ca. 200nm is typical. Because the confocal aperture admits light from only a specific plane of interest, thin optical sections can be resolved, giving a z resolution of less than 1μm, by changing the depth of the focal plane within the sample. Because the 2D x-y plane images are obtained in digital form, a series of successive optical sections can be analyzed with commercially available image analysis software to create 3D reconstructions or perform complex measurements. These powerful features offer opportunities for the study of micropipe dimension and morphology.

Figures 1(a) and (b) show SWBXT images recorded in back-reflection and transmission geometries, respectively, from a basal plane sample polished to a thickness of ca. 150μm. These figures show the overall distribution of defects in the crystals. Figures 2(a) and 2(b) show in detail a small indicated area of the wafer in figure 1. The main features observable on the back reflection images ($\mathbf{g}$=(00024), λ=1.25Å) consist of black rings with white centers of various diameters that are associated with the surface intersections of superscrew dislocations of various sized Burgers vectors ($\mathbf{b}$).[6,7] In addition to the larger Burgers vector superscrew dislocations (greater than about $\mathbf{b}$=3$\mathbf{c}$) that are associated with micropipes, indicated by **P**, there are many smaller circular features, **p**, that have no corresponding micropipes observable by fluorescence microscopy. The transmission SWBXT images

Downloaded by [Tomsk State University of Control Systems and Radio] at 10:39 18 February 2013

($\mathbf{g}=(10\bar{1}1)$, $\lambda=1.40$Å) show dark dots corresponding to the positions of superscrew dislocations and their associated micropipes. The dark dots are the origins of swirling networks of dislocations, **D**, following and with Burgers vectors lying in the basal plane.

In the conventional optical microscopy of the basal-cut 6H-SiC sample impregnated with fluorescent epoxy, the view of the micropipes through the (0001) face is of pink circular or oval cross-sections where they intersect the surface, with dark lines trailing downward into the crystal. Figure 2(c) shows a detail from a conventional optical micrograph of the same small indicated area of the wafer shown in figure 1. The red dye impregnating the micropipes has made them much more prominent, appearing as black lines in this figure. Some optical distortion in the crystal is visible around the micropipes. Figure 2(d) shows a fluorescence micrograph, taken without the use of confocal image processing, of the same area. It has been our experience that LSCM of a sample in this geometry is not useful below a depth of ca. 4μm below the sample surface, because of self-shadowing by the higher layers of the dyed micropipes,[20] therefore, we have limited our observations to the plane of focus at the wafer's surface. Micropipes, **P**, appear as bright specks against a dark matrix of SiC. The cross section of the emergent micropipes appear as circles or ellipses filled with fluorescence. The fluorescent columns of the micropipes that lie below the plane of focus appear as halos surrounding the bright specks, which aid in their identification. The shapes and diameters of the cross-sections of these micropipes can be determined with a good degree of accuracy in this geometry. It is typical for individual micropipes to be resolved as clusters of several micropipes, sometimes connected intermittently by microfissures. In the specimens examined here, no micropipes below 0.6μm in diameter were observed, although the lower limit for this method should be a micropipe of ca. 0.2μm diameter. However, SEM imaging of as-grown surfaces has revealed micropipes down to diameters of 0.1-0.2μm[16] so that the observations reported here may simply reflect the statistical distribution of defects in the particular samples examined.

Figure 3 shows views of a micropipe in a portion of the same wafer cut along the $(10\bar{1}0)$ plane. It can be seen that such longitudinal-cut samples can provide more extensive information with these techniques. Figure 3(a) is an optical micrograph, showing that the pink dye-filled micropipe runs the length of the pale green sample (micropipes appear as gray on a white background in figure 3(a)) . In contrast to the limitations of LSCM in a basal plane view, the LSCM image in figure 3(b) gives information about the entire length of the micropipe, which appears white on

a black background in this figure. The diameter of the micropipe varies from 0.8 to 1.4μm along its length. Along the lengths of these micropipes, there are areas of no fluorescence, possibly indicating the presence of particles, perhaps crystallites, lodged inside. The SWBXT image (g=(0006), λ=0.65Å) in figure 3(c) is sensitive only to displacement components associated with the micropipes which lie in the axial direction. The contrast of such images of superscrew dislocations, obtained from longitudinal sections of crystal, is bimodal, consisting of two dark lines on either side of the dislocation core which have relative displacements of opposite

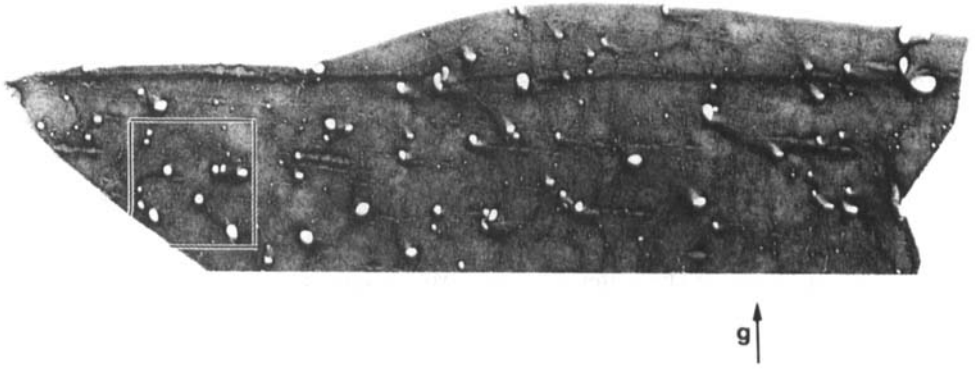

(a)

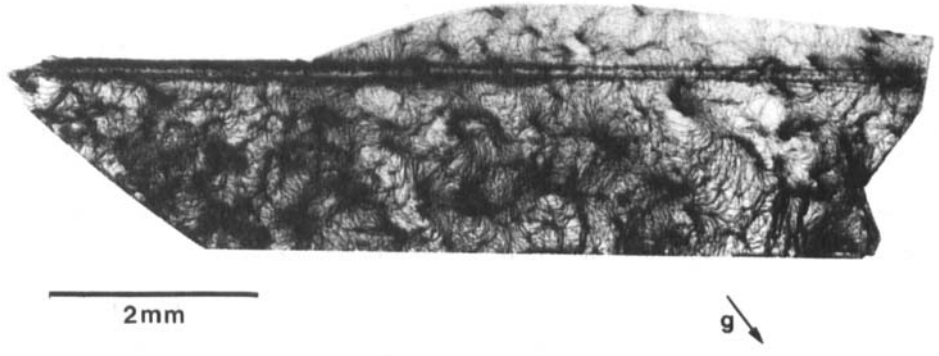

(b)

FIGURE 1. SWBXT images recorded from a basal plane wafer polished to a thickness of ca. 150μm: (a) Back-reflection image (g=(00024), λ=1.25Å); (b) Transmission image (g=(10$\bar{1}$1), λ=1.40Å).

Downloaded by [Tomsk State University of Control Systems and Radio] at 10:39 18 February 2013

Downloaded by [Tomsk State University of Control Systems and Radio] at 10:39 18 February 2013

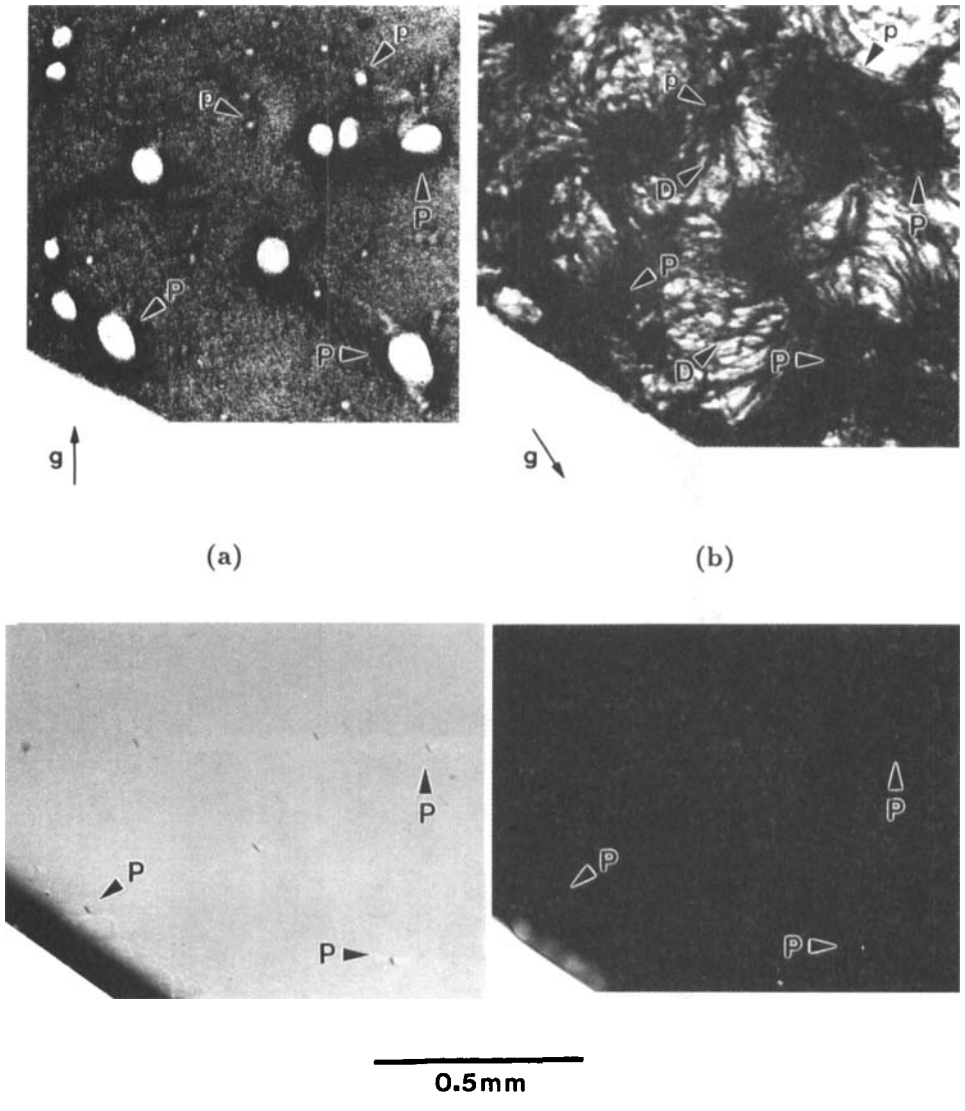

FIGURE 2. Details from superscrew dislocation images recorded from the area indicated in figure 1(a): (a) Back-reflection topograph; (b) Transmission topograph; (c) Conventional optical micrograph; (d) Fluorescence micrograph.

sign in the axial direction. This relative displacement is expected for screw dislocations and can be used to determine the sign and magnitude of the

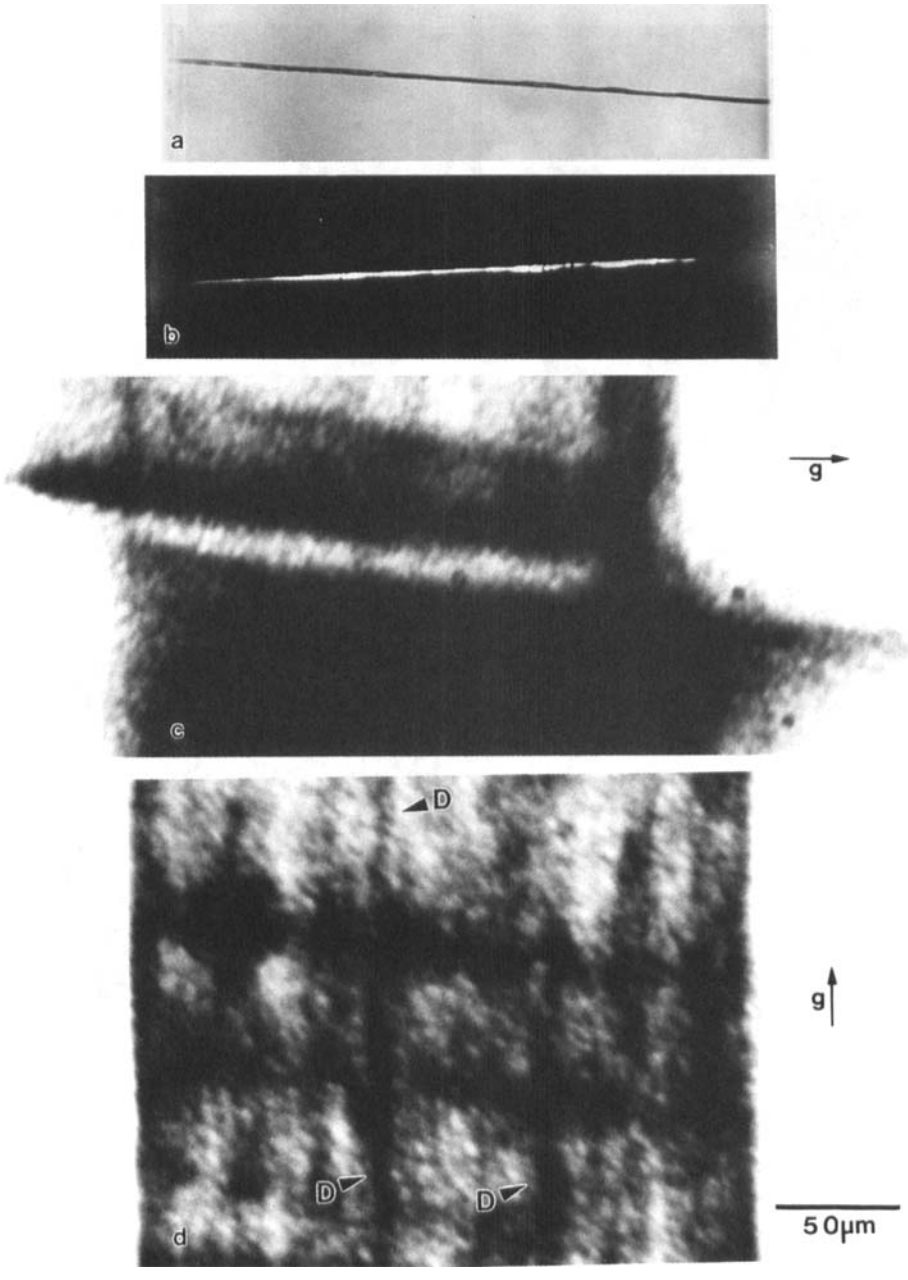

FIGURE 3. Superscrew dislocation images recorded from a longitudinal-cut SiC wafer: (a) Optical micrograph; (b) Laser scanning confocal micrograph; (c) Transmission topograph, $\mathbf{g}=(0006)$, $\lambda=0.65$Å; (d) Transmission topograph, $\mathbf{g}=(11\bar{2}0)$,$\lambda=0.64$Å.

Downloaded by [Tomsk State University of Control Systems and Radio] at 10:39 18 February 2013

Downloaded by [Tomsk State University of Control Systems and Radio] at 10:39 18 February 2013

Burgers vector.[4,18] Figure 3(d) is a SWBXT image of a reflection ($\mathbf{g}=(11\bar{2}0)$, $\lambda=0.64$Å) whose **g** vector lies in the basal plane. This image is again sensitive only to components of displacement which are parallel to the reflection vector. In this image, the contrast of the superscrew dislocation image arises largely from the surface strains on the micropipe cavity. Dislocations, **D**, with Burgers vectors lying in the basal plane are periodically emitted from the superscrew dislocations along the length of the micropipe. The strain contrast from the dislocations appears strongest at the points where the dislocations are emitted. Comparison of figure 2(b) with figure 2(d), shows that the micropipes periodically dilate and constrict along their lengths, and that the periodicity of these diameter fluctuations appears to be the same as that of the emission of basal plane dislocations. This may be interpreted using the notion that, at the growth temperature of an SiC crystal, basal plane dislocation loops are periodically emitted to partially relieve stress at various places along the length of a superscrew dislocation.[4,5] Following partial relaxation of the stress by basal plane dislocation emission, the local strain energy of the micropipe is reduced, changing the local equilibrium between strain energy and surface energy of the micropipe, ultimately enabling the micropipe to decrease its diameter. This underlines the importance of taking measurements of micropipe diameter at various positions along the length of the micropipe, and shows that modifications have to be introduced to the Frank relationship between micropipe diameter and Burgers vector.[10,19]

CONCLUSIONS

(1) SWBXT readily reveals superscrew dislocations in 6H-SiC single crystals, as well as providing details on surrounding microstructural features such as basal plane dislocations.

(2) After staining with fluorescent dye doped epoxy, LSCM reveals the position, size and shape of the micropipes that lie at the cores of these superscrew dislocations. The staining also renders them much more visible in conventional optical microscopy.

(3) The superscrew dislocation strain fields appear to be greatest where basal plane dislocations are emitted. Micropipes are observed to periodically dilate and constrict along their lengths, and the periodicity of these diameter fluctuations appears to be the same as that of the emission of basal plane dislocations. This suggests that the two phenomena may be related.

ACKNOWLEDGEMENTS

Research Supported by the U.S. Army Research Office under contract numbers DAAH04-94-G-0091 and DAAH04-94-G-0121 (contract monitor Dr. John T. Prater). Topography carried out at the Stony Brook Synchrotron Topography Facility, Beamline X-19C, at the NSLS, which is supported by the U.S. Department of Energy. We wish to thank T.-F. Wong and D. E. Colflesh for helpful discussion.

REFERENCES

1. A.R. Verma, Crystal Growth and Dislocations, (Academic Press, New York, 1953).
2. S. Mardix, A.R. Lang, and I. Blech, Phil. Mag., 24, 683 (1971).
3. A.P. Krishna, S.-S. Jiang, and A.R. Lang, J. Cryst. Growth, 71, 41 (1985).
4. S. Wang, M. Dudley, C. Carter, Jr., D. Asbury, and C. Fazi, in Applications of Synchrotron Radiation Techniques to Materials Science, Mat. Res. Soc. Symp. Proc., 307, 249 (1993).
5. S. Wang, M. Dudley, C.H. Carter, Jr., and H.S. Kong, in Diamond, SiC, and Nitride Wide Bandgap Semiconductors, Mat. Res. Soc. Symp. Proc., 339, 735, (1994).
6. S. Wang, M. Dudley, C.H. Carter, Jr., V. Tsvetkov, and C. Fazi, in Applications of Synchrotron Radiation Techniques to Materials Science II, Mat. Res. Soc. Symp. Proc., 375, 281, (1995).
7. M. Dudley, S. Wang, W. Huang, C.H. Carter, Jr., V.F. Tsvetkov, and C. Fazi, J. Phys. D: Appl. Phys., 28, A63 (1995).
8. F.C. Frank, Disc. Faraday Soc., 5, 48 (1949).
9. F.C. Frank, Phil. Mag., 42, 1014 (1951).
10. F.C. Frank, Acta Cryst., 4, 497, (1951).
11. E. Alexander, Z.H. Kalman, S. Mardix, and I.T. Steinberger, Phil. Mag., 21, 1237, (1970).
12. J.P. Golightly, Zeit. Krist., 130, 310, (1969).
13. H. Tanaka, Y. Uemura and J. Inomata, J. Crystal Growth, 53, 630, (1981).
14. H. Komatsu and S. Miyashita, Jpn. J. Appl. Phys., 32, 1478, (1993).
15. I. Sunagawa and P. Bennema, J. Crystal Growth, 53, 490, (1981).
16. M. Dudley, W. Si, W.M. Vetter and S. Wang, to be published, (1995).
17. Y. Inomata, H. Komatsu, M. Mitomo, and Z. Inoue, J. Crystal Growth, 2, 322, (1968).
18. J.T. Fredrich, B. Menéndez and T.-F. Wong, Science, 268, 276, (1995).
19. M. Dudley and W.M. Vetter, to be published, (1995).
20. P.C. Cheng and R.G. Summers, in J.B. Pawley, Handbook of Biological Confocal Microscopy, (Plenum Press, New York, 1990), p.179.

Downloaded by [Tomsk State University of Control Systems and Radio] at 10:39 18 February 2013